Short communication

The effect of a ceria coating on the H$_2$S tolerance of a molten carbonate fuel cell

Hary Devianto, Sung Pil Yoon *, Suk Woo Nam, Jonghee Han, Tae-Hoon Lim

Fuel Cell Research Center, Korea Institute of Science & Technology, 39-1 Hawolgok-dong, Seongbuk-gu, Seoul 136-791, Republic of Korea

Abstract

To enhance the performance of anodes in molten carbonate fuel cells (MCFCs), in terms of their sulfur tolerance, we modified the surface characteristics of a conventional Ni–10 wt% Cr anode through dip coating using a ceria sol. The performance of the ceria-coated anode was 0.4 V higher than that of the uncoated anode when H$_2$S (80 ppm) was introduced under a current density of 150 mA cm^{-2} for 180 h. H$_2$S acted as a poison of the non-modified Ni electrode, regardless of its operating conditions, to form Ni$_3$S$_2$, which caused the voltage drop. The ceria-coated anode had the ability to suppress such a voltage drop because ceria can react with H$_2$S to form Ce$_2$O$_2$S. Our results suggest that the presence of a CeO$_2$ coating layer can reduce the degree of sulfur poisoning of the anode under the operating conditions – e.g., a reducing atmosphere and a high temperature – experienced by MCFCs.
© 2005 Elsevier B.V. All rights reserved.

Keywords: MCFC; Anode; Surface modification; Wettability; Sulfur; Ceria

1. Introduction

The heart of most efficient power generation systems in the near future will be fuel cells that use hydrogen as their fuel. Considering fuel costs and infrastructure, however, hydrocarbon fuels will most likely be used as the hydrogen source in the early stages of the fuel cell era. In this context, molten carbonate fuel cells (MCFCs) possess the advantage of internally reforming the hydrocarbon fuels because MCFCs are operated at a high temperature (650 °C). Most raw hydrocarbon fuels that can be used in MCFC systems contain impurities (e.g., sulfur compounds) that are harmful to both the MCFC anode and the reforming catalyst. It is well established that even low-parts-per-million concentrations of sulfur compounds in fuel gases are detrimental to MCFCs. The principal sulfur compound that causes adverse effects on cell performance is H$_2$S. At anodic potentials, nickel anodes react with H$_2$S to form nickel sulfide, which can block active electrochemical reaction sites [1]:

$$H_2S + CO_3^{2-} \rightarrow H_2O + CO_2 + S^{2-} \tag{1}$$

$$Ni + xS^{2-} \rightarrow NiS_x + 2xe^- \tag{2}$$
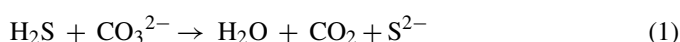
The tolerance of MCFCs to sulfur compounds depends strongly on the temperature, pressure, gas composition, cell components, and the mode of system operation (e.g., recycling, venting, and gas cleanup).

Two general processes are used to remove sulfur-containing compounds from fuels: hydro-desulfurization (HDS) and absorption. An HDS system must be designed so that the fuel gas passing through the fuel cell stacks contains only very low levels of sulfur (typically below 0.1 ppm). If the fuel cell plant has a source of hydrogen-rich gas (usually from the reformer exit), it is a common practice to recycle a small amount of this gas back into the HDS reactor. In this reactor, any organic sulfur-containing compounds are converted, over a supported nickel molybdenum oxide or cobalt molybdenum oxide catalyst, into hydrogen sulfide through hydrogenolysis reactions. The H$_2$S that is formed from such reactions is subsequently absorbed onto a bed of zinc oxide to form zinc sulfide. Undesirable hydro-cracking reactions can occur over HDS catalysts, which reduce their efficiency. HDS as a means of removing sulfur to very low levels is ideally suited to the proton exchange membrane (PEM) or phosphoric acid fuel cell (PAFC) systems. Unfortunately, HDS cannot be applied readily to internal reforming molten carbonate fuel

cell or solid oxide fuel cell (SOFC) systems because there is no hydrogen-rich stream that can be fed into the HDS reactor. Most developers of such systems have, therefore, replaced the HDS process for the removal of sulfur from the feed gases with the use of an absorbent. Activated carbons and molecular sieves are usually used as absorbent systems for fuel cells, but their absorption capacities are quite low and, thus, they are often used in sizeable amounts, which may be a serious economic disadvantage for large systems [2]. If the anode itself had a high tolerance toward sulfur impurities, the sulfur-removal process could be scaled down or eliminated to reduce the capital costs of the MCFC plant. In this study, we analyzed the use of ceria coatings on the anode in an attempt to enhance its sulfur tolerance.

2. Experimental

2.1. Surface modification of anode through ceria sol–gel coating

The conventional MCFC anode that was used was a highly porous sintered-nickel powder of the "chain" morphology type (INCO #255), alloyed with chromium. It was prepared through a procedure involving tape casting, drying, and calcination of a slurry mixture of solvent (water), binder (methyl cellulose #1500; Junsei Chemical Co., Japan), plasticizer (glycerol; Junsei Chemical Co., Japan), defoamer (SN-154; San Nopco, Korea), deflocculant (cerasperse-5468; San Nopco, Korea), and Ni powder (INCO #255; particle size: 3 μm), as reported previously [3]. The coating solution was prepared by mixing ceria sol (Alfa; 20% colloidal dispersion in H_2O) and ethanol (99.9%, Hayman) in a 1:2 weight ratio. Several dip coatings were performed to obtain a suitable coating ratio for a high-performance anode displaying a high sulfur tolerance. The anode was dipped into the ceria sol solution for several seconds, dried at 50 °C for 24 h in air, and then subjected to calcination at 700 °C for 30 min in a 5% H_2/N_2 atmosphere.

2.2. Cell operation

To analyze the effect that sulfur had on cell performance, a single cell (10 cm × 10 cm) was used. The experimental conditions and characteristics of the unit cell operation are summarized in Table 1. The prepared samples were placed in the heating block with cathode, electrolyte, matrix, current collector, and cell frame to form a single molten carbonate fuel cell. A pressure of 2 kgf (cm^{-2}) was applied to the unit cell using a cylinder of air. Operation of a single cell having a 10 cm × 10 cm anode was performed after pre-treatment at temperatures from 25 to 450 °C for 3 days in air and then from 450 to 650 °C for 3 days under CO_2. Under the latter conditions, which were very critical to electrolyte melting region, CO_2 was passed through the system at a low flow rate to maintain the distribution of the electrolyte throughout the pores of the matrix, cathode, and anode and also to prevent evaporation of the electrolyte.

After pretreatment, the temperature of the gas in the MCFC was maintained at 650 °C for 180 h, followed by H_2S being

Table 1
Conditions and characteristics of single-cell operation

Unit cell components	Values and characteristics
Cell frame of anode and cathode	
Size (width × length; cm × cm)	13 × 13
Material	Aluminized SUS–316
Anode electrode and current collector	
Size (width × length; cm × cm)	11 × 11
Thickness (mm)	ca. 0.75
Porosity	55–60%
Pore size (μm)	3–4
Material (electrode; current collector)	Ni–10 wt% Cr, CeO_2 coating; Ni
Mole ratio of fuel gas (H_2:CO_2:H_2O)	72:18:10
Total flow rate	365 mL min^{-1}
Cathode electrode and current collector	
Size (width × length; cm × cm)	10 × 10
Thickness (mm)	ca. 0.65
Porosity	60–65%
Pore size (μm)	7–8
Material (electrode; current collector)	In situ lithiated NiO; SUS 316
Mole ratio of oxidant gas (Air:CO_2)	70:30
Total flow rate	950 mL min^{-1}
Electrolyte	
Li_2CO_3/K_2CO_3 mole ratio	62:38
Matrix	γ-LiAlO$_2$

introduced at 80 ppm for 180 h, and then the system was returned back to normal gas. The anode gas consisted of H_2, CO_2, and H_2O in a 72:18:10 mole ratio; the cathode gas consisted of air and CO_2 in a 70:30 mole ratio. During the introduction of H_2S, the I–V curve was measured under H_2S concentrations in the range 0–100 ppm, the upper limit being 10 times higher than the concentration an anode can tolerate [1]. The total operating time was more than 450 h. The open circuit voltage (OCV), the performance, the internal resistance, and the N_2 cross-over were all measured during cell operation. Out-of-cell tests using a mixture of H_2 and H_2S as the anode input gas were performed to investigate the effect of the presence of a sulfur impurity.

2.3. Microstructure analysis

Several different analysis techniques were employed to examine the characteristics of the prepared samples. The surface morphology and the cerium and sulfur depth distributions of the porous Ni–10 wt% Cr anode were explored using scanning electron microscopy (SEM; Philips XL30 ESEM) in conjunction with energy dispersive spectrometry (EDAX). The phase structures and the structure of the compound produced were characterized using an X-ray diffractometer (XRD, Rigaku RINT-5200), equipped with a thin film attachment, and Cu Kα radiation. To compensate for the translation and dilation of X-ray peaks, silicon powder (single-crystal wafer; space group: Fd3m) was spread onto the surface of the electrodes. The pore size distribution was analyzed using a Hg porosimeter (Micromeritics Autopore IV). The surface area was measured using a Micromeritics ASAP 2000 instrument. The porosity of the sample was calculated using the Archimedes principle (ASTM C373-88).

3. Results and discussion

3.1. Morphology of the modified anode

Coating the surface of a nickel anode with a thin oxide layer from a ceria sol (particle diameters: ca. 10 nm) can provide the advantage of good wettability between the electrolyte and the anode. We used SEM to investigate the surface morphologies of the coated and uncoated anodes after the samples had been dried for 24 h at 50 °C and then heat treated for 30 min at 700 °C. Fig. 1 shows SEM images of the surface of the prepared anode. We applied several coatings to maintain a good distribution of CeO_2 particles within the anode pores. We used cerium mapping through EDAX to investigate the CeO_2 depth distributions within the porous anodes. The number of ceria particles in the pores increased upon increasing the number of dipping cycles. The anode pore sizes decreased as a result of the ceria layers covering the pore surfaces. Moreover, when the coating ratio was above 3 wt%, the ceria particles blocked the pores so that the sol solution could not infiltrate into the center of the anode. As a result (Fig. 2), ceria particles accumulated readily on the surface

when the coating ratio of above 3 wt%. The two main parameters that were considered to determine the optimum coating ratio were degree of dispersion and wettability. At 2 wt%, the ceria showed uniform dispersion along the cross-section of the anode and had the highest wettability of all of the samples. In regard to electrical conductivity, because the oxide film is resistive, excess oxide coating on the surface can reduce the electrical conductivity of the anode. Direct electrical conductivity measurements were not made, but can be inferred from the sample's superior performance.

Structural stability of the coating film is an important requirement to avoid undesirable microstructure changes and electrolyte loss through reactions with the electrolyte. We performed XRD analyses to examine the phase stability of ceria in molten carbonate eutectics. From the XRD patterns in Fig. 3, we observe peaks for ceria only; no other products appeared after the operating conditions were applied for 200 h. This finding suggests that no reaction occurred between the ceria and either the Li/K or Li/Na electrolyte.

3.2. Sulfur tolerance when H_2 was used as a fuel

The slopes of the initial I–V curves in Fig. 4 increase upon increasing the H_2S content, whereas under the initial state (open circuit voltage) conditions they remained the same. These phenomena occurred for both the non-modified and CeO_2-coated anodes. For both the Ni–10 wt% Cr and CeO_2/Ni–10 wt% Cr anodes, the output dry gases, which we analyzed using gas chromatography (GC), comprised H_2, N_2, CO, and CO_2 in a 75.6:0.5:16.4:7.5 ratio. Under the OCV conditions, the voltage remained constant upon increasing the H_2S concentration because nickel sulfide was not formed. This result is consistent with that reported by Uchida et al. [4], who performed kinetic studies of the effects that H_2S impurities have on the oxidation of hydrogen in molten $(Li + K)_2CO_3$; according to Selman and Maru [5], these phenomena are a result of the physical adsorption of H_2S onto the electrode surfaces. For the non-modified anode, in contrast, the voltage loss was larger than that for the CeO_2-coated anode [cf. Fig. 4(a and b)]. In the case of the non-modified anode, the addition of H_2S in the range 60–100 ppm caused the slope to increase more abruptly. We observed a similar phenomenon for the CeO_2-coated anode, but the degree of performance degradation was smaller than that of the non-modified anode. For example, adding H_2S at 80 ppm to the H_2 fuel led to the decreased performances of the single cells incorporating both the non-modified and CeO_2-coated anodes (Fig. 5). Even though the performance decreased upon adding H_2S to the fuel, the cells remained stable during their operation for 180 h. The voltage loss was suppressed to below 0.1 V, however, in the cell operated with the CeO_2-coated anode. It displayed better performance than did the pure Ni–10 wt% Cr anode, which exhibited a voltage loss of over 0.4 V at a current density of 150 mA cm^{-2}. When the H_2S was withdrawn from the anode gas, the performance of the cell incorporating the CeO_2-coated anode returned to normal [Fig. 5(b)]. In contrast, the performance of the non-modified anode did not recover fully, especially under high current densities [Fig. 5(a)].

Acc.V Spot Magn Det WD   500 nm
15.0 kV 3.0 50000x SE 7.7 KIST NMRC

(a)

Acc.V Spot Magn Det WD   500 nm
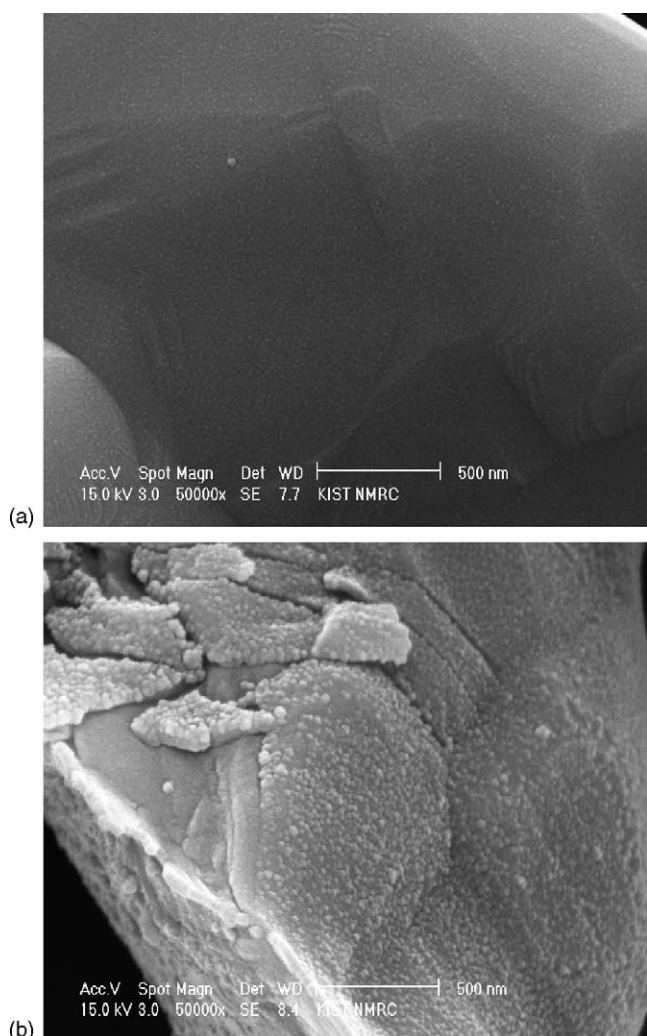15.0 kV 3.0 50000x SE 8.4 KIST NMRC

(b)

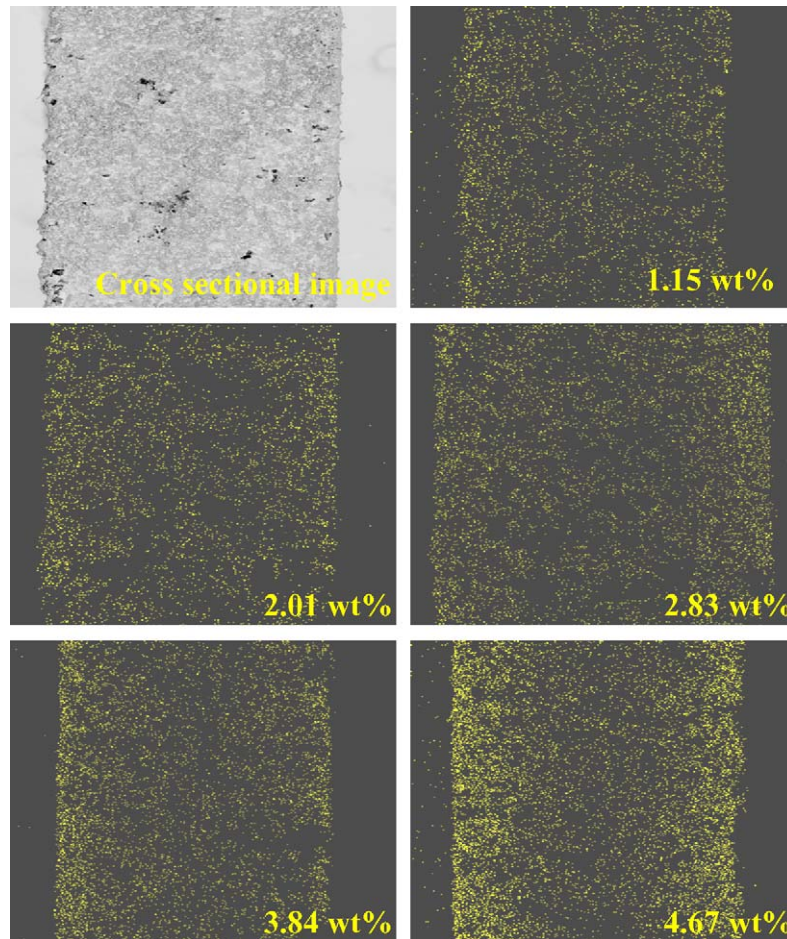Fig. 1. SEM images of Ni surfaces (a) before and (b) after coating with ceria.

Fig. 2. Uniform distributions of cerium throughout the ceria-coated Ni–10 wt% Cr anodes.

It is well known that CeO_2 has the ability to remove H_2S, especially under a reducing atmosphere and at high temperature [6]. Harrison et al. [7] reported that, under a reducing atmosphere, CeO_2 can be reduced to non-stoichiometric CeO_n ($n < 2$) that has a significantly greater affinity for H_2S. According to Yi [6], CeO_2 is a good candidate for use as a primary desulfuriza-tion sorbent to lower the H_2S concentration from 1% to several hundred parts per million; a zinc-based sorbent can then be used to reduce the H_2S concentration from several hundred to several parts per million. This process was analyzed through a study of thermodynamics and preliminary experimental results. It is well known that CeO_2 reacts with H_2S through the following equation:

$$2CeO_{2(s)} + H_{2(g)} + H_2S_{(g)} \rightarrow Ce_2O_2S_{(s)} + 2H_2O_{(g)} \qquad (3)$$

It has also been reported that at a temperature of 800 °C for a Ce–O–S system, coal gas desulfurization would likely result in the formation of oxysulfide (Ce_2O_2S) – not sulfide – in addition to other candidate sorbents. From the phase stability diagram, we note that the formation of Ce_2S_3 from CeO_2 is favored only when the partial pressure of sulfur is very high and that of oxygen is extremely low; Ce_2O_2S is the more likely sulfidation prod-uct. We also note that whereas the direct conversion of CeO_2 to Ce_2O_2S is possible only over narrow ranges of sulfur and oxygen pressures, reduced cerium oxide (CeO_{2-x}) is more readily con-verted to Ce_2O_2S. In fact, Ce_2O_3 should be capable of removing H_2S to extremely low levels through the following reaction:
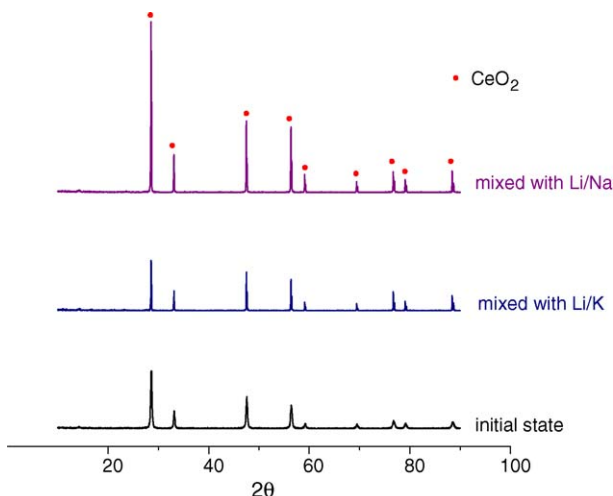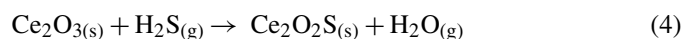
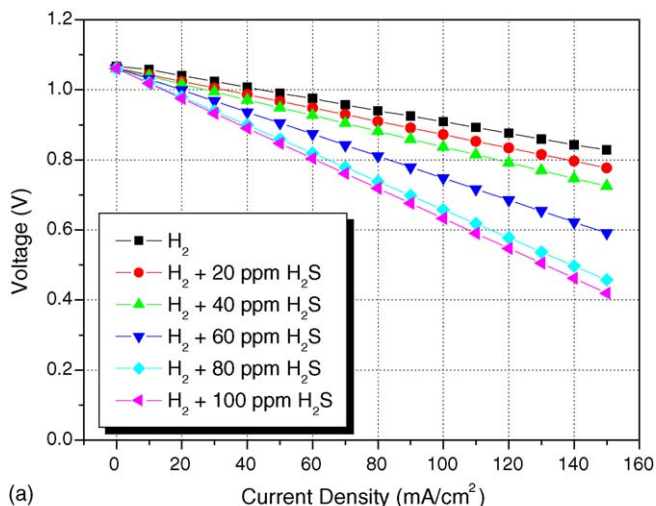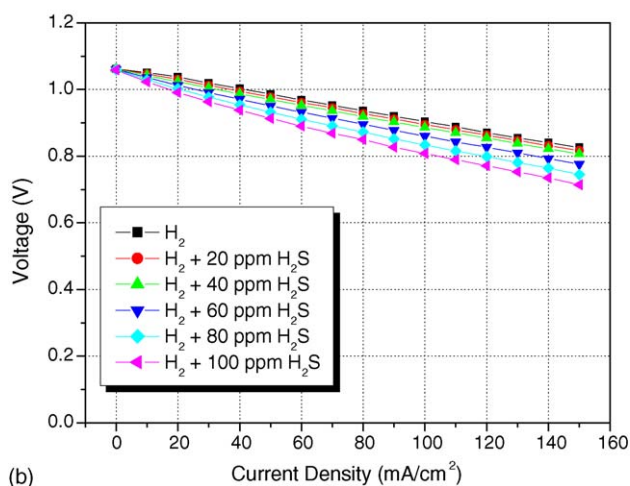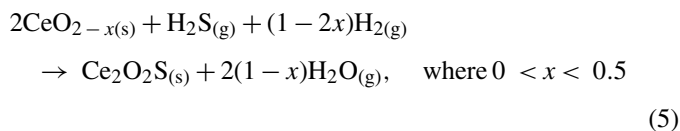$$Ce_2O_{3(s)} + H_2S_{(g)} \rightarrow Ce_2O_2S_{(s)} + H_2O_{(g)} \qquad (4)$$

Fig. 3. XRD patterns of ceria.

(a)

(b)

Fig. 4. Initial I–V curves of the (a) pure Ni–10 wt% Cr and (b) CeO2-coated anodes when using hydrogen as the fuel.

(a)

(b)

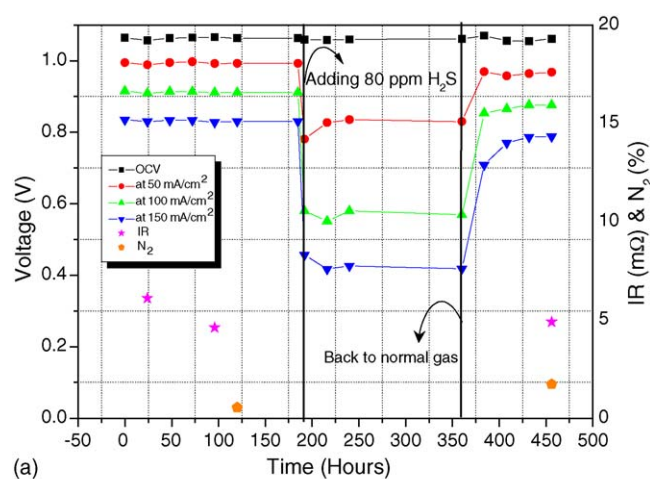Fig. 5. Performance curves of the (a) pure Ni–10 wt% Cr and (b) CeO2-coated anodes when using hydrogen as the fuel.

The partial pressure of oxygen required to form Ce_2O_3, however, is extremely low ($<10^{-26}$); i.e., it is much lower than the value of P_{O_2} in an actual sample of coal gas. Thus, it has been suggested that partially reduced CeO_2 be used, as represented by the following equation:

$$2CeO_{2-x(s)} + H_2S_{(g)} + (1-2x)H_{2(g)}$$
$$\rightarrow Ce_2O_2S_{(s)} + 2(1-x)H_2O_{(g)}, \quad \text{where } 0 < x < 0.5$$
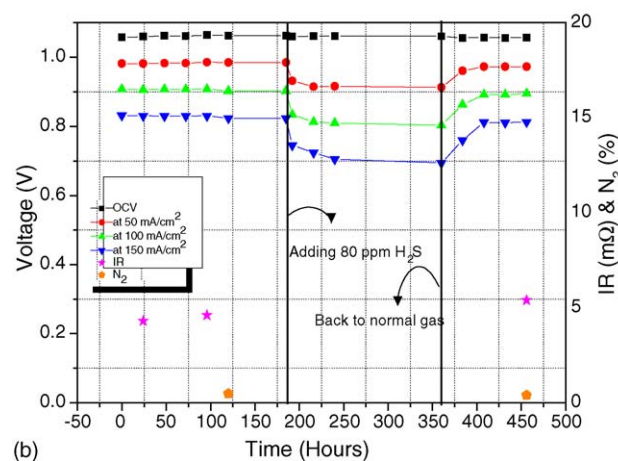
(5)

Therefore, we believe that the ceria layers formed by sol–gel coating of the anode behave as a sulfur sorbent through the formation of oxysulfide (Ce_2O_2S) as described in reaction (5). Consequently, the cell incorporating the CeO_2-coated anode displays improved sulfur tolerance and performance relative to that incorporating the unmodified anode.

We used XRD to characterize the anode samples after their exposure to H_2S in an effort to identify the sulfide compounds that formed; Fig. 6 provides a comparison of the various samples. Because the intensity of the nickel peak was dominant over a wide range of values of 2θ (from 0 to 50°), the other peaks
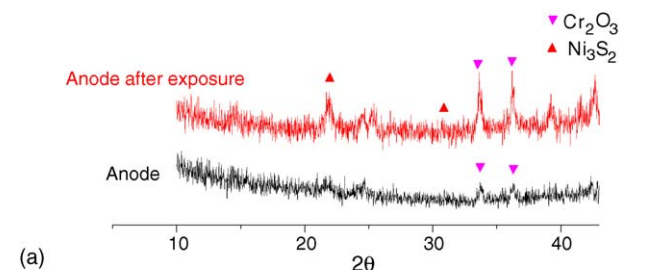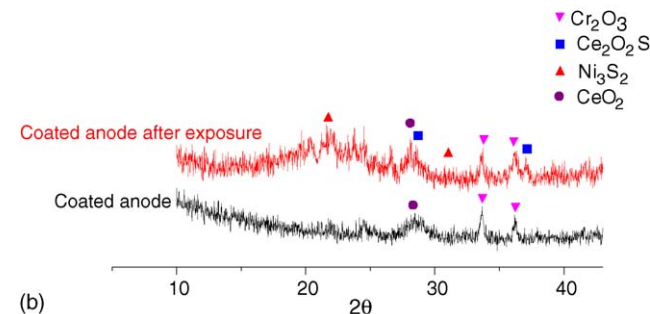

(a)

(b)

Fig. 6. XRD data for the (a) pure Ni–10 wt% Cr and (b) CeO2-coated anodes when using hydrogen as the fuel.

were magnified in the range of 2θ from 0 to $45°$ by removal of the nickel peak. In contrast to the XRD signals of the unmodified samples, the modified anode presented a ceria peak at $28.5°$. When both the pure Ni–10 wt% Cr and CeO_2-coated anode samples were exposed to H_2S during cell testing, their nickel anodes reacted with sulfur to form a nickel sulfide, Ni_3S_2; Nowak et al. [8] reported a similar result from their study of the corrosion effects of Ni/Cr alloys in H_2S/H_2 mixtures at temperatures between 600 and $900°C$. In contrast, the CeO_2-coated anode also formed ceria oxysulfide (Ce_2O_2S) through the mechanism described above. Consequently, it is clear that the different performances exhibited in Figs. 4 and 5 occur as a result of the formation of ceria oxysulfide, which acts as a sulfur absorbant. In addition, no cerium deposition occurred on the anode during its operation at $650°C$, irrespective of the presence of H_2S.

4. Conclusion

From cell tests with the modified anodes, the ceria was uniformly distributed through the cross-sectional area of the anode. The ceria sols having small particle sizes (diameter: ca. 10 nm) created thin layers of ceria on the Ni surface. This surface modification led to increased wettability and no reaction occurred between the ceria and the electrolyte. The Ni-based anode was poisoned by H_2S to form Ni_3S_2, which caused a voltage drop. In contrast, the ceria-coated anode exhibited a suppressed voltage drop under the operating conditions because the ceria reacted with H_2S to form Ce_2O_2S, a sulfur sorbent. Furthermore, the coated anode obstructed any sintering phenomena from occurring because its surface was covered and scattered with ceramic material through a pinning effect. Since this is the initial study related with thin film oxide to protect sulfur poisoning, additional experiments, such as coating with different materials, modifying the anode base material, and performing tests for longer durations, should be conducted to enhance the anode properties to achieve high-performance MCFCs suitable for long-term operation.

References

[1] A.J. Appleby, F.R. Foulkes, Fuel Cell Handbook, sixth ed., Krieger, New York, 1992.
[2] J. Larminie, A. Dicks, Fuel Cell Systems Explained, John Wiley & Sons, Singapore, 2000, pp. 189-190.
[3] J.H. Wee, D.J. Song, C.S. Jun, T.H. Lim, S.A. Hong, H.C. Lim, K.Y. Lee, J. Alloys Compd. 390 (2005) 155–160.
[4] I. Uchida, S. Ohuchi, T. Nishina, J. Electroanal. Chem. 369 (1994) 161–168.
[5] J.R. Selman, H. Maru, Proceedings of the Third Symposium on MCFC Technology, Electrochemical Society, 1993, p. 186.
[6] K.B. Yi, Ph.D. Thesis, Louisiana State University, 2004.
[7] D.P. Harrison, E.J. Podlaha, K.B. Yi, High Efficiency Desulfurization of Synthesis Gas: III, Final Report, Louisiana State University 2003.
[8] J.F. Nowak, M. Lambertin, J.C. Colson, Corros. Sci. 18 (1978) 971–982.